

# A new measurement method for electrode gain in an orthogonally symmetric beam position monitor<sup>\*</sup>

ZOU Jun-Ying(邹俊颖)<sup>1)</sup> WU Fang-Fang(吴芳芳) YANG Yong-Liang(杨永良) SUN Bao-Gen(孙葆根)<sup>2)</sup>  
 ZHOU Ze-Ran(周泽然) LUO Qing(罗箐) LU Ping(卢平) XU Hong-Liang(徐宏亮)

NSRL, School of Nuclear Science and Technology University of Science and Technology of China, Hefei 230029, China

**Abstract:** The new beam position monitor (BPM) system of the injector at the upgrade project of the Hefei Light Source (HLS II) has 19 stripline beam position monitors. Most consist of four orthogonally symmetric stripline electrodes. Differences in electronic gain and mismatching tolerance can cause changes in the beam response of the BPM electrodes. This variation will couple the two measured horizontal positions, resulting in measuring error. To alleviate this effect, a new technique to measure the relative response of the four electrodes has been developed. It is independent of the beam charge, and the related coefficient can be calculated theoretically. The effect of electrode coupling on this technique is analyzed. The calibration data is used to fit the gain for all 19 injector beam position monitors. The results show the standard deviation of the distribution of measured gains is about 5%.

**Key words:** beam position monitor, electrode gain, calibration, orthogonal symmetric

**PACS:** 29.20.Ej, 29.90.+r **DOI:** 10.1088/1674-1137/38/12/127002

## 1 Introduction

The Hefei Light Source (HLS) is currently being upgraded to HLS II. The injector beam position monitoring (BPM) system is composed of 19 beam position monitors, most of which are regular stripline type BPMs. They are precisely calibrated and carefully installed in place [1]. We have developed a new technique that provides a measure of the relative gain of the four stripline electrodes.

The method we developed is similar to the technique of D. L. Rubin [2] et al. It also based on the fact that, in a four electrodes beam position monitor, the position of the beam is overdetermined. The relative gains of the electrodes can be calculated by measuring the electrode signal at many different beam positions. Rubin's method is based on image theory, which requires the geometry of the four BPM electrodes to be diagonally symmetric. The geometry of a typical HLS II beam position monitor is as shown in Fig. 1. The four electrodes are orthogonally symmetric, for which Rubin's method does not apply, so we have developed a new technique to measure the relative gains for this type of four-electrode beam position monitor. Through the analysis of the the-

oretical electrode signal induced by the beam, we find a new expression related only to the electrode signal. This expression can be used to fit the electrode gain errors. For each fitting procedure, four unknown parameters are fitted: three button gains and a geometry scaling factor.

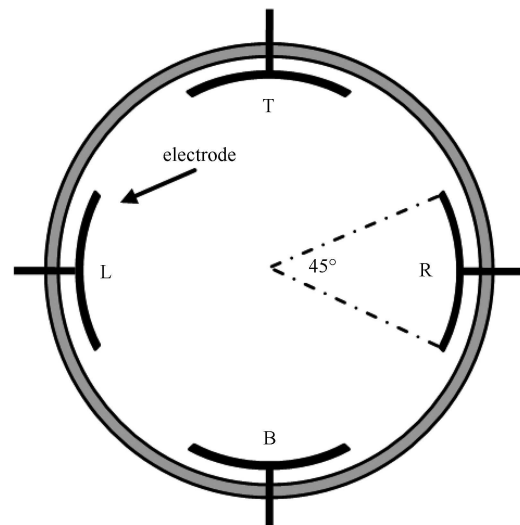


Fig. 1. HLS II injector beam position monitor.

Received 2 January 2014, Revised 3 March 2014

<sup>\*</sup> Supported by National Natural Science Foundation of China (11175173, 11375178, 11105141)

1) E-mail: zoujyyl@mail.ustc.edu.cn

2) E-mail: bgsun@ustc.edu.cn

©2014 Chinese Physical Society and the Institute of High Energy Physics of the Chinese Academy of Sciences and the Institute of Modern Physics of the Chinese Academy of Sciences and IOP Publishing Ltd

## 2 Derivation of new expression

As Fig. 1 shows, the four electrodes of a HLS II typical BPM are 90 degrees away from each other. By ignoring the influence of bunch size, the electrode signal of this type of BPM can be represented by [3]

$$\begin{cases} V_R = \frac{I_{\text{beam}}\phi}{2\pi b} (1 + Z_{1x} + Z_2 + Z_{3x} + Z_4 + \dots), \\ V_L = \frac{I_{\text{beam}}\phi}{2\pi b} (1 - Z_{1x} + Z_2 - Z_{3x} + Z_4 + \dots), \\ V_T = \frac{I_{\text{beam}}\phi}{2\pi b} (1 + Z_{1y} - Z_2 - Z_{3y} + Z_4 + \dots), \\ V_B = \frac{I_{\text{beam}}\phi}{2\pi b} (1 - Z_{1y} - Z_2 + Z_{3y} + Z_4 + \dots), \end{cases} \quad (1)$$

where  $I_{\text{beam}}$  is the beam charge,  $\phi$  is the opening angle of the electrodes, and  $b$  is the distance from the center of the beam position monitor to the electrodes.  $Z_{1x}$ ,  $Z_{1y}$ ,  $Z_2$ ,  $Z_{3x}$ ,  $Z_{3y}$  and  $Z_4$  are introduced in order to simplify the expressions to

$$\begin{cases} Z_{1x} = 2 \frac{\sin(\phi/2)}{\phi/2} \frac{x_0}{b}, & Z_{1y} = 2 \frac{\sin(\phi/2)}{\phi/2} \frac{y_0}{b}, \\ Z_2 = 2 \frac{\sin\phi}{\phi} \frac{x_0^2 - y_0^2}{b^2}, \\ Z_{3x} = 2 \frac{\sin(3\phi/2)}{3\phi/2} \frac{x_0^2 - 3y_0^2}{b^2} \frac{x_0}{b}, \\ Z_{3y} = 2 \frac{\sin(3\phi/2)}{3\phi/2} \frac{3x_0^2 - y_0^2}{b^2} \frac{y_0}{b}, \\ Z_4 = \frac{\sin(2\phi)}{\phi} \frac{3(x_0^2 - y_0^2)^2 - 2(x_0^4 + y_0^4)}{b^4}. \end{cases} \quad (2)$$

where  $x_0$  and  $y_0$  are the positions of the beam. When the beam is near the center of the beam pipe,  $x_0$  and  $y_0$  are small compared to  $b$ . In this case, the third order and up can be ignored, so the electrode signals can be approximated as a quadratic polynomial expansion

$$\begin{cases} V_R = \frac{I_{\text{beam}}\phi}{2\pi b} (1 + Z_{1x} + Z_2), \\ V_T = \frac{I_{\text{beam}}\phi}{2\pi b} (1 + Z_{1y} - Z_2), \\ V_L = \frac{I_{\text{beam}}\phi}{2\pi b} (1 - Z_{1x} + Z_2), \\ V_B = \frac{I_{\text{beam}}\phi}{2\pi b} (1 - Z_{1y} - Z_2). \end{cases} \quad (3)$$

Taking the sums and differences of Eq. (3) gives

$$\begin{cases} E_Q = \frac{V_R + V_L - (V_T + V_B)}{V_R + V_L + V_T + V_B} = Z_2, \\ E_{x-y} = \frac{V_R - V_L - \frac{V_T - V_B}{V_R + V_L}}{V_R + V_L} = \frac{Z_{1x} - Z_{1y} - Z_2 Z_{1x} - Z_2 Z_{1y}}{1 - Z_2 Z_2}, \\ E_{x+y} = \frac{V_R - V_L + \frac{V_T - V_B}{V_R + V_L}}{V_R + V_L} = \frac{Z_{1x} + Z_{1y} - Z_2 Z_{1x} + Z_2 Z_{1y}}{1 - Z_2 Z_2}, \end{cases} \quad (4)$$

where  $E_Q$  is the electrical quadrupole component signal,  $E_{x-y}$  is the electrical position signal of  $x$  minus  $y$ ,  $E_{x+y}$  is the electrical position signal of  $x$  plus  $y$ . Also, ignoring the third order and up we can simply get

$$\begin{cases} E_Q = Z_2, \\ E_{x-y} = Z_{1x} - Z_{1y}, \\ E_{x+y} = Z_{1x} + Z_{1y}. \end{cases} \quad (5)$$

Combining Eq. (2) and Eq. (5) to eliminate  $x_0$  and  $y_0$  gives an expression that simply relates the electrode signals:

$$\begin{cases} E_Q = k E_{x-y} E_{x+y}, \\ k = \frac{\phi}{4 \tan(\phi/2)}. \end{cases} \quad (6)$$

In this case,  $k$  is a constant determined only by the electrode opening angle of the BPM. For a regular injector stripline BPM in HLS II,  $\phi$  is  $45^\circ$  and  $b=13.1$  mm, so we can simply calculate that  $k$  is 0.474. Eq. (6) not only shows that  $E_Q$  is proportional to the product  $E_{x-y} E_{x+y}$ , but more importantly, that the equation is irrelevant to the beam charge, which is useful when fitting the gain errors using real beam.

## 3 Simulation

To simulate the connection between  $E_Q$  and  $E_{x-y} E_{x+y}$ , we used a finite element code to create a map of each electrode response as a function of beam position [4].

The simulated beam was moved in a  $10 \text{ mm} \times 10 \text{ mm}$  square area with a step of 0.5 mm.  $E_Q$  and  $E_{x-y} E_{x+y}$  were calculated with the exact response of electrodes at every beam position. The product  $E_{x-y} E_{x+y}$  is plotted versus  $E_Q$  in Fig. 2. In Fig. 2, only slight deviations from the straight line appear at large amplitudes, showing the extent to which the higher than second order terms can be ignored.

We see that our quadratic term approximation works well, with the product  $E_{x-y} E_{x+y}$  approximated to  $E_Q$ ,

fitting the form of Eq. (6) with only slight deviations at large amplitudes.

In practice, the four electrodes do not have the same gain, so the connection between electrodes defined by Eq. (6) will fail. We simulate the effect of gain errors by reducing the signal on electrode B by 10%. Fig. 3 shows  $E_{x-y}E_{x+y}$  vs  $E_Q$  with the data under this condition, with + indicating the coordinate origin (0,0). The data is no longer linear and it is offset from zero.

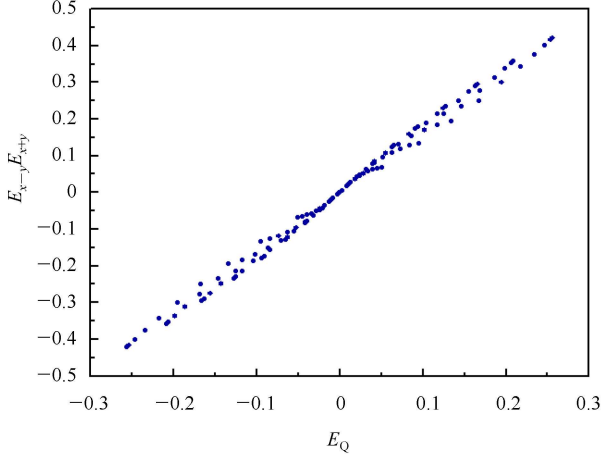


Fig. 2.  $E_{x-y}E_{x+y}$  vs  $E_Q$  for points on a 10 mm  $\times$  10 mm grid with simulated electrodes signal vs beam position.

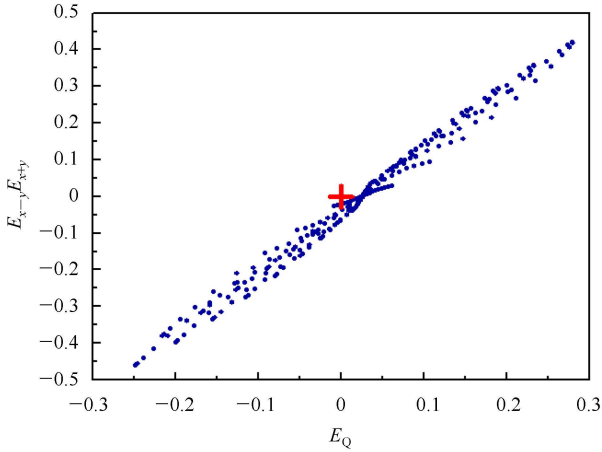


Fig. 3.  $E_{x-y}E_{x+y}$  vs  $E_Q$  for points on a 10 mm  $\times$  10 mm grid, with electrode intensity computed with the nonlinear map.

#### 4 Electrode coupling effect

Equation (6) is based on the assumption that the four electrodes are independent of each other. In fact, there is a coupling effect between the electrodes. Each electrode can be induced by signals from other electrodes. We set  $K_1$  as the coupling coefficient of the opposite electrode,

and  $K_2$  as the coupling coefficient of an adjacent electrode. So the four electrode signals are given by

$$\begin{cases} \tilde{V}_R = V_R + K_1 V_L + K_2 V_T + K_2 V_B, \\ \tilde{V}_L = K_1 V_R + V_L + K_2 V_T + K_2 V_B, \\ \tilde{V}_T = K_2 V_R + K_2 V_L + V_T + K_1 V_B, \\ \tilde{V}_B = K_2 V_R + K_2 V_L + K_1 V_T + V_B. \end{cases} \quad (7)$$

In this case, we calculate Eq. (4) by ignoring the third order and up

$$\begin{cases} \tilde{E}_Q = \frac{\tilde{V}_R + \tilde{V}_L - (\tilde{V}_T + \tilde{V}_B)}{\tilde{V}_R + \tilde{V}_L + \tilde{V}_T + \tilde{V}_B} = \frac{1 - 2K_2 + K_1}{1 + 2K_2 + K_1} Z_2, \\ \tilde{E}_{x-y} = \frac{\tilde{V}_R - \tilde{V}_L}{\tilde{V}_R + \tilde{V}_L} - \frac{\tilde{V}_T - \tilde{V}_B}{\tilde{V}_T + \tilde{V}_B} = \frac{(1 - K_1)(Z_{1x} - Z_{1y})}{(1 + 2K_2 + K_1)}, \\ \tilde{E}_{x+y} = \frac{\tilde{V}_R - \tilde{V}_L}{\tilde{V}_R + \tilde{V}_L} + \frac{\tilde{V}_T - \tilde{V}_B}{\tilde{V}_T + \tilde{V}_B} = \frac{(1 - K_1)(Z_{1x} + Z_{1y})}{(1 + 2K_2 + K_1)}. \end{cases} \quad (8)$$

So Eq. (6) can be modified to

$$\begin{cases} \tilde{E}_Q = \tilde{k} \tilde{E}_{x-y} \tilde{E}_{x+y}, \\ \tilde{k} \approx \frac{(1 + K_1)^2 - 4K_2^2}{(1 - K_1)^2} \frac{\phi}{4 \tan(\phi/2)}, \end{cases} \quad (9)$$

where  $\tilde{k}$  is a coefficient determined by the electrode coupling effect and the electrode opening angle. We calculate the coupling coefficients through analysis of the simulation BPM model using CST-Microwave Studio software. A simulated Gaussian signal is generated at one electrode. By integrating the original signal and the induced signal at other electrodes, we obtain  $K_1 = 1.82\%$  and  $K_2 = 5.52\%$ . Finally, we obtain  $\tilde{k}$  to be about 0.504.

#### 5 Electrode gain fit with new expression

We assume the deviations from Eq. (9) are determined by the gain variations between different electrodes. We use a nonlinear least squares fit to get the electrode gains ( $g_R$ ,  $g_L$ ,  $g_T$  and  $g_B$ ). The merit function to be minimized is

$$\chi^2 = \sum_{i=1}^n \left( \frac{g_R \tilde{V}_R + g_L \tilde{V}_L - (g_T \tilde{V}_T + g_B \tilde{V}_B)}{g_R \tilde{V}_R + g_L \tilde{V}_L + g_T \tilde{V}_T + g_B \tilde{V}_B} - \tilde{k} \left( \frac{g_R \tilde{V}_R - g_L \tilde{V}_L}{g_R \tilde{V}_R + g_L \tilde{V}_L} - \frac{g_T \tilde{V}_T - g_B \tilde{V}_B}{g_T \tilde{V}_T + g_B \tilde{V}_B} \right) \right)^2 \times \left( \frac{g_R \tilde{V}_R - g_L \tilde{V}_L}{g_R \tilde{V}_R + g_L \tilde{V}_L} + \frac{g_T \tilde{V}_T - g_B \tilde{V}_B}{g_T \tilde{V}_T + g_B \tilde{V}_B} \right) \quad (10)$$

$\chi^2$  has a minimum for the best fit gains ( $g_R$ ,  $g_L$ ,  $g_T$  and  $g_B$ ) and  $\tilde{k}$ . To make sure the value of the denominator is not zero, we fit the same data four times, each time

setting one of the electrode gains to 1, and then average the results.

### 6 Fitting the calibration data

All the 19 HLS II injector stripline BPMs are calibrated at a test bench, using a tungsten filament to simulate the beam [1]. The filament was moved in a 10 mm×10 mm square area with a step of 0.5 mm. We collected the electrodes signal data on each simulated beam position using Libera Brilliance Single Pass [5]. An example of fitted data based on Eq. (10) at one BPM (LA-BD-BPM03) is shown in Fig. 4. In Fig. 4, the open circles are the raw electrode data, the crosses are the electrode data corrected with the fitted gains, the + indicates the coordinate origin (0,0). The fitted gains ( $g_R$ ,  $g_L$ ,  $g_T$  and  $g_B$ ) are 0.882, 1.122, 0.923 and 1.122 respectively. The results show that the data has better linearity and passes through zero after gain fitting. The fitted gains have large differences, because we included the worst BPM, in which the mechanical processing quality is low (machining errors are visible even by the naked eye). This indicates that the gain fit is quite necessary.

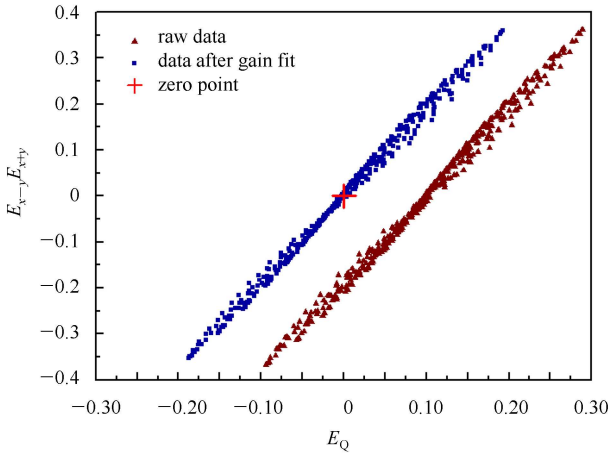


Fig. 4.  $E_{x-y} E_{x+y}$  vs  $E_Q$  for a calibration data at LA-BD-BPM03.

To verify the effectiveness of the above method, Table 1 shows the main changes in the geometric calibration parameters of LA-BD-BPM03 before and after gain fitting. Compared to the geometric coefficient before gain fitting, the geometric coefficient is closer to the theoretical value of 7.55 mm after gain fitting. Thus, the above method is effective.

The gains for all 19 BPMs are shown in Fig. 5. The distribution of fitted gains is shown in Fig. 6. The standard deviation of the distribution of measured gains is about 5%. Most electrodes gain errors are between 0.9 and 1.1. Note that the average value of parameter  $\tilde{k}$  is 0.530, which is a little bit larger than the theoretical value 0.504. The reason could be an increase in the

coupling effect caused by mechanical processing, and the calibration method.

Table 1. The change of calibration parameters before and after gain fitting.

position	before gain fitting		after gain fitting	
	$x$	$y$	$x$	$y$
offset/mm	-0.19	-0.15	-0.13	-0.01
geometric coefficient/mm	7.60	7.41	7.60	7.45

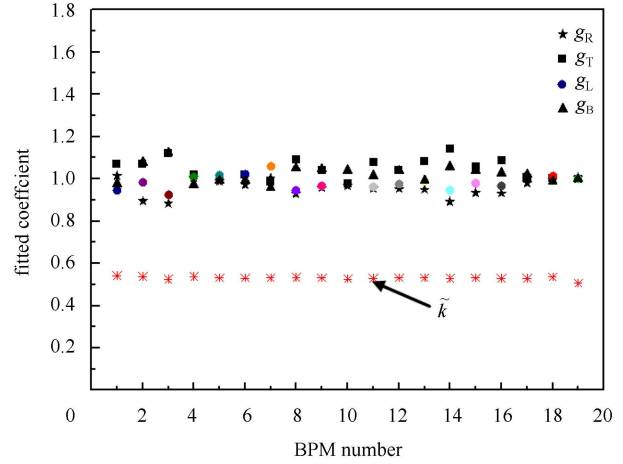


Fig. 5. Fitted gains and parameter  $\tilde{k}$  from calibration data for all 19 injector beam position monitors.

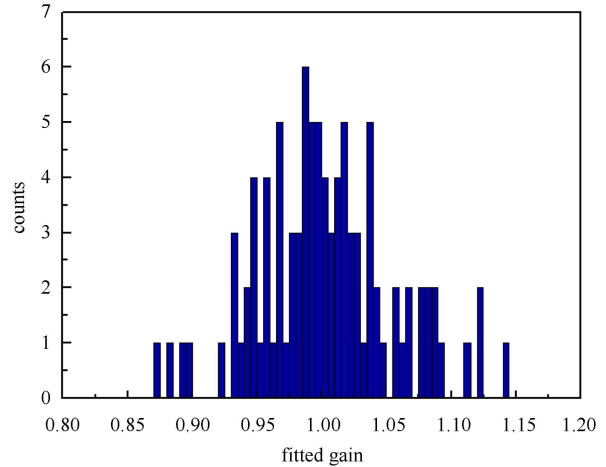


Fig. 6. Distribution of fitted gains for the data plotted in Fig. 5.

### 7 Simulation of real beam gain fit

The calibration beam is equally distributed in a 10 mm×10 mm square area, but the distribution of the real beam is not so equal. To see if the gain fit method is still effective, we perform a simulation of this situation.

Considering that the fit will be better when the beam is in a smaller range near the center, and the beam can be precisely controlled using corrector magnets, we simulate 50 random beam points in a 4 mm×4 mm square area. Also, because most electrodes gain errors are between 0.9 and 1.1, we reduce the signal of the electrode B by 10%, that is, the theoretical fitted gains (1:4)=0.9750, 0.9750, 0.9750, 1.0833. We fit the gains following the above procedure, giving fitted gains (1:4)=0.9749, 0.9745, 0.9752, 1.0839. The difference from the theoretical value is less than 0.1%. The  $E_{x-y}$   $E_{x+y}$  vs  $E_Q$  before and after gain fit is shown in Fig. 7.

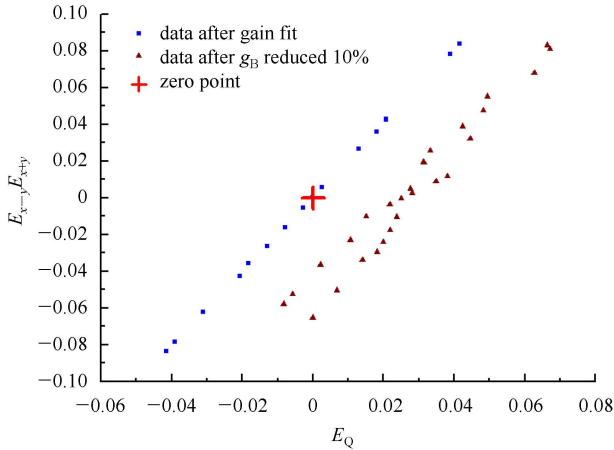


Fig. 7.  $E_{x-y}$   $E_{x+y}$  vs  $E_Q$  for 50 simulated beams in a 4 mm×4 mm square area.

In real beam gain fitting, we will try to control the beam as precisely as possible, making it move in a 4 mm×4 mm square area with a step of 0.5 mm. A total of 81 beam points are collected. The fitted results should be better than the previous simulation due to larger sampling number and more equal distribution of the beam.

## 8 Conclusion

We have derived a relationship between the intensities of the four electrodes of an orthogonal symmetrical type beam position monitor. This relationship is better than those derived in previous studies because it is independent of the beam charge and the related coefficient can be theoretically calculated. We analyze the effect of electrode coupling on the relationship. We also show how the relationship can be used to make a beam-based measurement of the relative gains of the four electrodes. We have used the calibration data to fit the gain for all 19 injector beam position monitors. The standard deviation of the distribution of measured gains is about 5%, consistent with the specifications of the system electronics. A simulation of real beam gain fit with this method is done, showing the difference from the theoretical value to be less than 0.1%. In future, will use real beam data from the HLS II injector to fit the electrode gain; this can be implemented as a part of the standard measurement suite of the HLS II injector BPM system.

## References

- 1 ZOU Jun-Ying, YANG Yong-Liang, SUN Bao-Gen et al. Calibration of Beam Position Monitors in the Injector of HLS II. Proceedings of IPAC2013. Shanghai, China, 2013. 568–570
- 2 Rubin D L, Billing M, Meller R et al. Phys. Rev. ST Accel. Beams, 2010, **13**(9): 092802-1–092802-6
- 3 LI Peng, SUN Bao-gen, LUO Qing et al. High Power Laser and Particle Beams, 2008, **20**(4): 573–578
- 4 Olmos A, Pérez F, Rehm G. Matlab Code for BPM Button Geometry Computation. Proceedings of DIPAC 2007. Venice, Italy, 2007. 186–188
- 5 ZOU Jun-Ying, FANG Jia, SUN Bao-Gen, et al. Application of Libera Brilliance Single Pass at NSRL Linac BPM System. Proceedings of IPAC2011. San Sebastián, Spain, 2013. 1284–1286